

# Synthesis, characterization and catalytic activity of supported molybdenum Schiff base complex as a magnetically-recoverable nanocatalyst in epoxidation reaction

Zeinab Moradi-Shoeili, Maryam Zare, Mojtaba Bagherzadeh, Saim Özkar & Serdar Akbayrak

To cite this article: Zeinab Moradi-Shoeili, Maryam Zare, Mojtaba Bagherzadeh, Saim Özkar & Serdar Akbayrak (2016): Synthesis, characterization and catalytic activity of supported molybdenum Schiff base complex as a magnetically-recoverable nanocatalyst in epoxidation reaction, Journal of Coordination Chemistry, DOI: [10.1080/00958972.2015.1137290](https://doi.org/10.1080/00958972.2015.1137290)

To link to this article: <http://dx.doi.org/10.1080/00958972.2015.1137290>



Accepted author version posted online: 06 Jan 2016.



Submit your article to this journal [↗](#)



Article views: 2



View related articles [↗](#)



View Crossmark data [↗](#)

**Publisher:** Taylor & Francis

**Journal:** *Journal of Coordination Chemistry*

**DOI:** <http://dx.doi.org/10.1080/00958972.2015.1137290>

## **Synthesis, characterization and catalytic activity of supported molybdenum Schiff base complex as a magnetically–recoverable nanocatalyst in epoxidation reaction**

ZEINAB MORADI–SHOEILI\*<sup>1</sup>, MARYAM ZARE<sup>2</sup>, MOJTABA BAGHERZADEH<sup>3</sup>, SAIM ÖZKAR<sup>4</sup> and SERDAR AKBAYRAK<sup>4</sup>

<sup>1</sup>Department of Chemistry, Faculty of Sciences, University of Guilan, P.O. Box 41335–1914, Rasht, Iran

<sup>2</sup>Materials Science & Engineering Department, Golpayegan University of Technology, P.O. Box 8771765651, Golpayegan, Iran

<sup>3</sup>Department of Chemistry, Sharif University of Technology, Azadi Ave., P.O. Box 11155–3516, Tehran, Iran

<sup>4</sup>Chemistry Department, Middle East Technical University, 06800 Ankara, Turkey

A heterogeneous nanocatalyst was prepared via covalent anchoring of dioxomolybdenum(VI) Schiff base complex on core–shell structured Fe<sub>3</sub>O<sub>4</sub>@SiO<sub>2</sub>. The properties and the nature of the surface–fixed complex have been identified by a series of characterization techniques such as SEM, EDX, XRD, TGA, FT–IR and VSM. The synthesized hybrid material was an efficient nanocatalyst for selective oxidation of olefins to corresponding epoxides with t–BuOOH in high yields and selectivity. The catalyst could be conveniently recovered by applying an external magnetic field and reused several times without significant loss of efficiency.

*Keywords:* Molybdenum complex; Magnetic nanoparticles; Heterogeneous catalyst; Schiff base; Epoxidation reaction

### **1. Introduction**

Epoxidation of alkenes and arenes is important in organic synthesis and industrial production due to its applications in the manufacturing of a variety of valuable materials [1, 2]. Design and fabrication of a catalyst with high selectivity, stability and recyclability is challenging. Among

---

\*Corresponding author. Email: zmoradi@guilan.ac.ir

the many transition metal complexes used as catalysts for selective epoxidation reactions [3-6], molybdenum(VI) compounds with Schiff base ligands have been intensively investigated as efficient homogeneous catalysts [7-10]. In most cases, the recovery of these kinds of catalysts from the reaction medium is extremely difficult and associated with environmental pollution [6, 11, 12]. As a result, heterogenizing of the catalytically active species to the surface of traditional solid supports has attracted attention [13-15]. However, immobilization of the homogeneous systems usually decreases the catalytic site accessibility for the substrate and consequently reduces the catalytic activity [16]. Hence, providing new types of heterogeneous catalysts that have an elevated rate of reaction and can be easily recovered from the reaction medium is ongoing [17-20].

Magnetite  $\text{Fe}_3\text{O}_4$  nanoparticles have attracted interest as support materials due to their low toxicity, high saturation magnetization and biocompatibility [21, 22]. Unprotected magnetic nanoparticles are found to be unstable and easily aggregate during catalytic transformations, resulting in deduction of magnetic properties, catalytic capability and dispersibility [23]. An approach which could effectively solve these problems is protecting the magnetic nanoparticles with a non-magnetic and chemically stable shell such as silica [24-26]. In addition, the outer shell of silica could be easily functionalized with various ligands which can also provide efficient binding sites to numerous catalytic species including transition metal complexes [13, 27]. Therefore, silica-coated magnetic nanoparticles ( $\text{Fe}_3\text{O}_4@ \text{SiO}_2$ ), as supports, have attracted interest to provide magnetically reusable heterogeneous catalysts [16, 28-30].

In this study, the synthesis and structural characterization of a new core-shell structured nanomaterial  $\text{Fe}_3\text{O}_4@ \text{SiO}_2\text{-NHAlMo}$  are described. The catalytic properties of the nanocatalyst were investigated in the epoxidation of olefins using *t*-BuOOH as oxygen source, which exhibited excellent catalytic performance with high yields and selectivity, mild reaction conditions and short reaction times. The catalyst could be conveniently separated using an external magnet and efficiently recovered several times without a significant loss in catalytic activity.

## 2. Experimental

### 2.1. Materials and methods

Air-sensitive operations were carried out using standard techniques under a nitrogen atmosphere. All reagents were obtained from commercial sources and used as received. Bis(acetylacetonato) dioxomolybdenum(VI),  $[\text{MoO}_2(\text{acac})_2]$  [31] was prepared as described in the literature.  $\text{Fe}_3\text{O}_4$  magnetite nanoparticles [32] and silica-coated  $\text{Fe}_3\text{O}_4$  ( $\text{Fe}_3\text{O}_4@\text{SiO}_2$ ) [33] were prepared following the previously published procedure. Powder X-ray diffraction (PXRD) data were collected with a Philips X'Pert MPD diffractometer (Co-K $\alpha$  [au: please check] X-radiation,  $\lambda = 1.79 \text{ \AA}$ ). The metal loading of the host materials and leaching of molybdenum into the solution were determined by inductively coupled plasma atomic emission spectroscopy (ICP-AES) on a Perkin-Elmer AA-300 spectrophotometer. FT-IR spectra of samples as KBr pellets were recorded using an ABB Bomem MB-100 FT-IR spectrophotometer; FT-IR spectra from catalytic studies were taken using a Unicam Matson 1000 FT-IR spectrophotometer. Scanning electron microscopy (SEM) images were taken on a KYKY-EM3200 scanning electron microscope. TGA and DTA analyses were carried out with a Thermo Gravimetric System Mettler Toledo TGA/DSC1 at a heating rate of  $5 \text{ }^\circ\text{C min}^{-1}$  under air. Elemental analysis was recorded with an energy dispersive X-ray (EDX) analyzer (KEVEX Delta series) mounted on the Hitachi S-800. A vibration sample magnetometer (VSM) was used to measure the magnetic properties of the samples at room temperature. Ni was used as a standard. Gas chromatographic (GC) analyses were performed on an Agilent Technologies 6890N, 19019 J-413 HP-5, 5% phenyl methyl siloxane, capillary column  $60.0\text{m}\times 250 \mu\text{m}\times 1.00 \mu\text{m}$ .

### 2.2. Synthesis of the $\text{Fe}_3\text{O}_4@\text{SiO}_2\text{-NH}_2$

The core-shell  $\text{Fe}_3\text{O}_4@\text{SiO}_2$  nanospheres were modified with 3-aminopropyltriethoxysilane (APTES) according to the procedure described previously [34]. 1 g of prepared  $\text{Fe}_3\text{O}_4@\text{SiO}_2$  nanoparticles was sonicated in 100 mL dry toluene for 30 min to achieve a uniform dispersion. Subsequently, 1 mL of APTES was added under vigorous stirring at room temperature for 24 h. The solid material was washed by toluene and ethanol several times and dried in an oven at  $70 \text{ }^\circ\text{C}$  for 8 h.

### **2.3. Synthesis of $Fe_3O_4@SiO_2-NHAl$**

Supported Schiff base was prepared by addition of 5-bromo salicylaldehyde (0.4 g, mmol) to a mixture of  $Fe_3O_4@SiO_2-NH_2$  (1 g) in ethanol (100 mL). The resultant mixture was refluxed for 24 h. The product was magnetically separated and washed with hot ethanol several times to remove unreacted species and dried at 70 °C for 6 h. This product will be referred as  $Fe_3O_4@SiO_2-NHAl$ .

### **2.4. Synthesis of $Fe_3O_4@SiO_2-NHAlMo$ nanoparticles**

260 mg of  $MoO_2(acac)_2$  was dissolved in 50 mL ethanol and  $Fe_3O_4@SiO_2-NHAl$  (0.4 g) was then added to this solution. The resultant mixture was refluxed for 24 h. The solid was magnetically separated and then washed several times with hot ethanol. The final product was dried in an oven at 70 °C for 8 h to afford supported molybdenum catalyst,  $Fe_3O_4@SiO_2-NHAlMo$ .

### **2.5. Catalytic reactions**

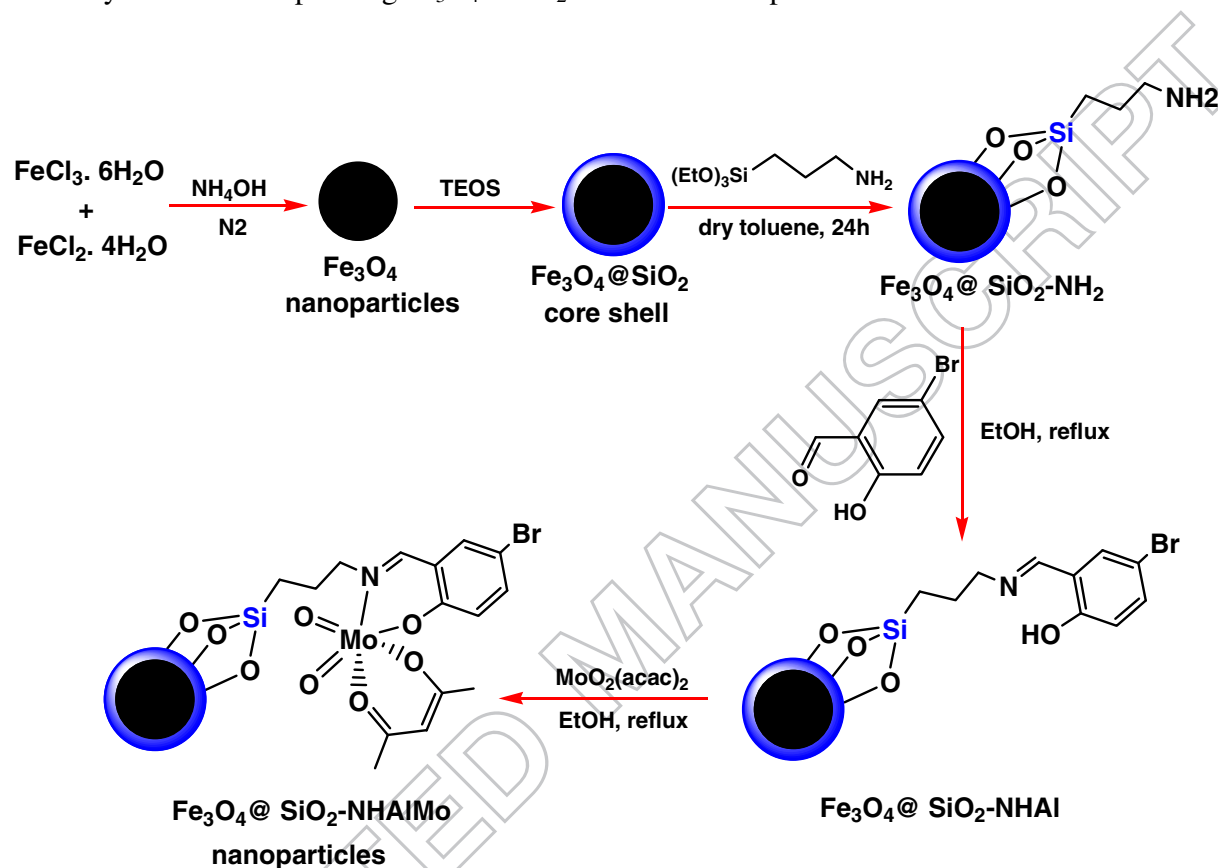
The liquid-phase olefin epoxidation reactions were carried out in air and autogenous pressure in a 5 mL batch micro-reactor equipped with a stir bar and a sampling valve, and immersed in a thermostated oil bath. Typically, a mixture of the substrate (1 mmol),  $Fe_3O_4@SiO_2-NHAlMo$  (10 mg), chlorobenzene (1 mmol) as internal standard and  $C_2H_4Cl_2$  (1 mL) was stirred in a 5 mL tube for 10 min at 84 °C. Then 182  $\mu$ L of 5.5 M solution of *t*-BuOOH in decane (1 mmol) was added and the system was stirred for 20-60 min under reflux. The progress of the reaction was monitored by GC. All the reactions were performed at least two times and the products were compared with standard samples.

## **3. Results and discussion**

### **3.1. Catalyst preparation and characterization**

The synthetic procedure for the  $Fe_3O_4@SiO_2-NHAlMo$  nanocomposite is illustrated in scheme 1. The magnetic  $Fe_3O_4$  nanoparticles of approximately 40 nm diameter were synthesized by co-precipitation method. In order to prevent decomposition and aggregation, magnetic nanoparticles were subsequently coated with a silica shell using tetraethoxysilane (TEOS) as the silica source. The silica layered system,  $Fe_3O_4@SiO_2$  was functionalized in two steps using

3-aminopropyltriethoxysilane (APTES) and 5-bromo salicylaldehyde (scheme 1) which affords suitable chelating Schiff base ligand for grafting of the molybdenum metal on the surface of the nanoparticles. Then, the prepared nanospheres were reacted with  $\text{MoO}_2(\text{acac})_2$  in ethanol for 24 h to yield the corresponding  $\text{Fe}_3\text{O}_4@ \text{SiO}_2\text{-NHAlMo}$  nanoparticles.



Scheme 1. Synthetic pathways for the synthesis of  $\text{Fe}_3\text{O}_4@ \text{SiO}_2\text{-NHAlMo}$  nanocomposite.

Figure 1 represents the FT-IR spectra of synthesized materials which are in agreement with the proposed structure shown in scheme 1. The FT-IR spectrum for  $\text{Fe}_3\text{O}_4$  nanoparticles (figure 1a) shows strong bands at  $3433$  and  $1623 \text{ cm}^{-1}$ , indicating water molecules adsorbed to the surface. Significant absorption at  $581 \text{ cm}^{-1}$  (evident in all spectra) and  $1061 \text{ cm}^{-1}$  (figures 1b, 1c and 1d) were attributed to stretching frequency of Fe-O and Si-O, respectively [35]. These peaks in FT-IR spectra reveal the formation of  $\text{Fe}_3\text{O}_4$  nanoparticles which were successfully coated with  $\text{SiO}_2$  layer. The sharp band at  $1635 \text{ cm}^{-1}$  (figure 1c) which was assigned to  $\nu(\text{C}=\text{N})$  has shifted to the  $1615 \text{ cm}^{-1}$  range (figure 1d) in the spectra of the complex suggesting coordination of nitrogen to molybdenum, in agreement with literature values [36, 37]. The band

at  $1539\text{ cm}^{-1}$  for  $\text{Fe}_3\text{O}_4@\text{SiO}_2\text{-NHAlMo}$  nanoparticles (figure 1d, inset) is not observed for  $\text{Fe}_3\text{O}_4@\text{SiO}_2\text{-NHAl}$ . This band could correspond to the vibration of the C=O group of acac, suggesting involvement of acac in coordination of molybdenum [38]. Two strong absorptions at  $903$  and  $939\text{ cm}^{-1}$  (figure 1d) are indicative of symmetrical and anti-symmetrical stretch of two *cis* doubly-bonded oxygens at the molybdenum core [39].

The structures of the  $\text{Fe}_3\text{O}_4$ ,  $\text{Fe}_3\text{O}_4@\text{SiO}_2\text{-NHAl}$  and  $\text{Fe}_3\text{O}_4@\text{SiO}_2\text{-NHAlMo}$  nanoparticles were determined by powder X-ray diffraction (XRD). As shown in figure 2, the diffraction patterns and relative intensities of all the peaks are in agreement with those of magnetite which can be indexed to the face-centered cubic phase of  $\text{Fe}_3\text{O}_4$  [23, 40, 41]. The broad peak between  $20\text{-}30^\circ$  in figures 2b and c indicates the amorphous structure of silica layer. In the XRD pattern of  $\text{Fe}_3\text{O}_4@\text{SiO}_2\text{-NHAl}$  and  $\text{Fe}_3\text{O}_4@\text{SiO}_2\text{-NHAlMo}$ , the characteristic peaks of  $\text{Fe}_3\text{O}_4$  did not change, revealing that the structure of  $\text{Fe}_3\text{O}_4$  is well maintained, after being coated with silica. No obvious reflections for  $\text{SiO}_2$  and Mo complex are observed, which indicates that they are relatively thin amorphous layers on the surface of  $\text{Fe}_3\text{O}_4$  nanospheres.

The morphology and sizes of  $\text{Fe}_3\text{O}_4$  and  $\text{Fe}_3\text{O}_4@\text{SiO}_2\text{-NHAlMo}$  were observed by scanning electron microscope (SEM).  $\text{Fe}_3\text{O}_4$  nanoparticles are relatively monodisperse particles with an average diameter of about  $40\text{ nm}$  (figure 3a). As shown in figure 3b, the nanocomposite particles were relatively uniform with a thickness of approximately  $50\text{ nm}$ , indicating the successful coating of silica around each magnetic  $\text{Fe}_3\text{O}_4$  core particle. Furthermore, SEM images showed that the nanoparticles still maintain their spherical shape after the coating procedures with silica and molybdenum complex. The EDX spectrum of  $\text{Fe}_3\text{O}_4@\text{SiO}_2\text{-NHAlMo}$  presented in figure 3c clearly demonstrates the presence of molybdenum in the composite. Using elemental microanalysis results (wt%) of the sample measured by EDX, the typical loading of the molybdenum moieties on the surface is  $0.79\text{ mmol/g}$ .

Thermogravimetric analysis of the  $\text{Fe}_3\text{O}_4@\text{SiO}_2\text{-NHAlMo}$  nanoparticle was carried out from  $25\text{-}800\text{ }^\circ\text{C}$  at a heating rate of  $10\text{ }^\circ\text{C min}^{-1}$  (figure 4). The complex showed weight losses at temperature below  $150\text{ }^\circ\text{C}$  that could be due to the removal of physically adsorbed water molecule and/or organic solvents which were adsorbed during the synthesis of nanoparticles. With further increase in temperature, the TG curves show two steps of weight loss. The first of  $1.52\%$  observed from  $200$  to  $260\text{ }^\circ\text{C}$  may be ascribed to desorption of the chemisorbed water on

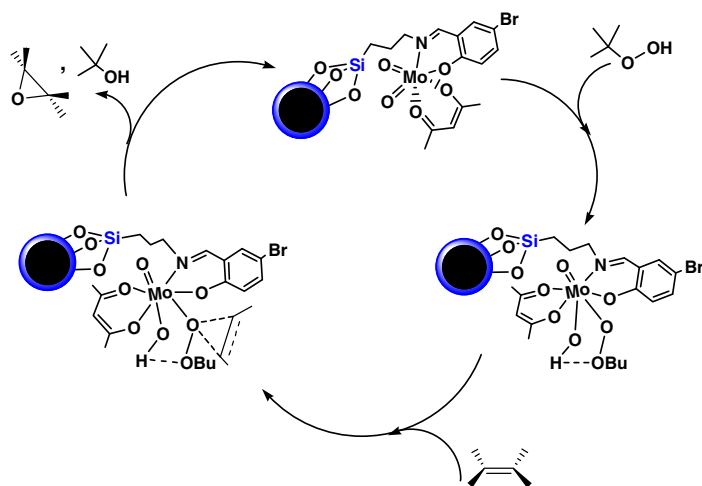
the silica surface [42]. At the last stage, the mass losses of 7.51% at 300–440 °C can be attributed to complete removal of the fragment parts of the ligand on the surface.

The magnetic properties of  $\text{Fe}_3\text{O}_4$  and the  $\text{Fe}_3\text{O}_4@\text{SiO}_2\text{-NHAlMo}$  nanocomposite were investigated using vibrating sample magnetometer (VSM) at room temperature in an applied magnetic field sweeping from –10 to 10 kOe. The magnetization curves of the samples are shown in figure 5. The absence of hysteresis phenomenon indicates that the magnetic particles have superparamagnetic behavior at room temperature. The results show that  $\text{Fe}_3\text{O}_4$  and  $\text{Fe}_3\text{O}_4@\text{SiO}_2\text{-NHAlMo}$  nanoparticles have saturated magnetization values of 61.0 and 45.6 emu/g, respectively. Compared with  $\text{Fe}_3\text{O}_4$  nanoparticles, a decrease of about 15.4 emu/g in saturation magnetization was observed for  $\text{Fe}_3\text{O}_4@\text{SiO}_2\text{-NHAlMo}$  nanocomposite which can be attributed to increase in mass and size after the coating of magnetite nanoparticles with silica and anchoring the Mo(VI) catalyst. Nevertheless, the final synthesized nanocatalyst can still be efficiently separated from the solution using an external magnet.

### 3.2. Catalytic epoxidation of olefins

Catalytic studies were initiated by testing the activity of  $\text{Fe}_3\text{O}_4@\text{SiO}_2\text{-NHAlMo}$  nanocatalyst in oxidation of cyclooctene using *t*-BuOOH as an oxidant. This reaction was best carried out using 10 mg catalyst and 1 mmol of *t*-BuOOH for 20 min under reflux in dichloroethane. The catalytic ability of the magnetite nanoparticle-supported catalyst was evaluated in catalyzing a series of olefins in the optimized conditions. As summarized in table 1, different alkenes are generally excellent substrates for these catalysts. The catalytic oxygenation of cyclohexene with *t*-BuOOH was carried out in the presence of material for 30 min under reflux. The selective conversion of cyclohexene to the corresponding epoxide indicates that the reaction proceeds via a non-radical mechanism [43, 44]. The least reactive aliphatic terminal alkenes such as *n*-octene and *n*-heptene were catalytically oxygenated in high yields and excellent selectivities. The olefins conjugated with a phenyl group such as  $\alpha$ -methylstyrene and 4-methylstyrene are converted into these epoxides in moderate yield. A proposed mechanism of the reaction is shown in scheme 2, postulated based on the result of the study and previously reported investigations by Thiel [16]. The catalytic reaction involves transfer of one *t*-BuOOH proton to one oxo group of dioxo complex and coordination of *t*-BuOO anion to the Lewis acidic metal center. Nucleophilic attack of an olefin to one oxygen of the peroxo ligand, as an electrophile, yields epoxide and *t*-butanol

as a by-product. The six-coordinate species is subsequently activated for oxygen transfer to the olefin.



Scheme 2. Proposed mechanism for oxidation of alkenes catalyzed by  $\text{Fe}_3\text{O}_4@\text{SiO}_2\text{-NHAlMo}$  in the presence of *t*-BuOOH.

The recyclability of the modified catalyst was examined by reusing the material isolated from a previous run in the next run of epoxidation of cyclooctene under the same conditions. For the reusability test, the catalyst was isolated from the reaction solution after complete epoxidation of cyclooctene by external magnet, washed with  $\text{C}_2\text{H}_4\text{Cl}_2$ , and dried at room temperature. The conversions at 20 min were similar for all six runs and selectivity to the epoxide remained very high (table 2). The leaching test was carried out after the catalyst was reused six times, the reaction mixture was filtered, and ICP measurement of the filtrate showed that no detectable molybdenum can be found, indicating that almost no leaching of the catalyst can be observed. In order to verify further whether the observed catalysis was truly heterogeneous, the solid was filtered off from the reaction mixture and the fresh alkene and oxidant was added to filtrate and no reaction was observed. Increase in the conversion in run 2 with respect to run 1 (table 2) could be attributed to trace amount of Mo(VI) leached from the catalyst into the solution.

The IR spectrum of  $\text{Fe}_3\text{O}_4$  supported catalyst before and after six reuses shows no major changes (figure 6). The spectrum contained medium intensity bands at  $2856$  and  $2976\text{ cm}^{-1}$ , attributed to *t*-butanol formed during the epoxidation process. The used catalyst may therefore

possess some active metal centers coordinated with t-butanol which could account for slight decrease in the olefin conversion rate.

Table 3 summarizes the comparison of catalytic activity of  $\text{Fe}_3\text{O}_4@\text{SiO}_2\text{-NHAlMo}$  in conversion of olefins to epoxides using t-BuOOH, with some of the reported molybdenum(VI) nanocatalysts. From these results, it is clear that  $\text{Fe}_3\text{O}_4@\text{SiO}_2\text{-NHAlMo}$  is more efficient and effective than other heterogeneous catalytic systems.

#### 4. Conclusion

Functionalized iron oxide nanoparticle was prepared and used as a support for immobilizing the dioxomolybdenum Schiff base complex. The catalytic activity of the prepared nanocatalyst was studied for selective oxidation of olefins to corresponding epoxides using t-BuOOH. The catalyst in olefin epoxidation reactions give high yield and selectivity of the products, in most cases. After completion of the reaction, the catalysts could be easily recovered by simple magnetic decantation. The heterogeneous nanocatalyst was chemically stable and can be reused at least six times with nearly constant catalytic activity; no metal leaching was detected after the consecutive catalytic reactions. Therefore, chemical stability, high activity, short reaction time, convenient recoverability and reusability make  $\text{Fe}_3\text{O}_4@\text{SiO}_2\text{-NHAlMo}$  nanocomposite a valuable catalyst in industrial applications.

#### References

- [1] Y. Zhu, Q. Wang, R.G. Cornwall, Y. Shi. *Chem. Rev.*, **114**, 8199 (2014).
- [2] O.A. Wong, Y. Shi. *Chem. Rev.*, **108**, 3958 (2008).
- [3] G. Licini, V. Conte, A. Coletti, M. Mba, C. Zonta. *Coord. Chem. Rev.*, **255**, 2345 (2011).
- [4] E.P. Talsi, K.P. Bryliakov. *Coord. Chem. Rev.*, **256**, 1418 (2012).
- [5] M. Amini, M.M. Haghdoost, M. Bagherzadeh. *Coord. Chem. Rev.*, **268**, 83 (2014).
- [6] B.S. Lane, K. Burgess. *Chem. Rev.*, **103**, 2457 (2003).
- [7] H. Vrabel, K.J. Ciuffi, G.P. Ricci, F.S. Nunes, S. Nakagaki. *Appl. Catal. A: Gen.*, **368**, 139 (2009).
- [8] M. Herbert, F. Montilla, A. Galindo. *J. Mol. Catal. A: Chem.*, **338**, 111 (2011).
- [9] M. Amini, M.M. Haghdoost, M. Bagherzadeh. *Coord. Chem. Rev.*, **257**, 1093 (2013).
- [10] A.J. Burke. *Coord. Chem. Rev.*, **252**, 170 (2008).

- [11] P.C. Bakala, E. Briot, L. Salles, J-M. Brégeault. *Appl. Catal. A: Gen.*, **300**, 91 (2006).
- [12] S.M. Bruno, J.A. Fernandes, L.S. Martins, I.S. Gonçalves, M. Pillinger, P. Ribeiro–Claro, João Rocha, A.A. Valente. *Catal. Today*, **114**, 263 (2006).
- [13] X. Zheng, L. Zhang, J. Li, S. Luo, J-P. Cheng. *Chem. Commun.*, **47**, 12325 (2011).
- [14] B. Monteiro, S.S. Balula, S. Gago, C. Grosso, S. Figueiredo, A.D. Lopes, A.A. Valente, M. Pillinger, J.P. Lourenço, I.S. Gonçalves. *J. Mol. Catal. A: Chem.*, **297**, 110 (2009).
- [15] U. Arnold, R. Serpa da Cruz, D. Mandelli, U. Schuchardt. *J. Mol. Catal. A: Chem.*, **165**, 149 (2001).
- [16] S. Shylesh, J. Schweizer, S. Demeshko, V. Schünemann, S. Ernst, W.R. Thiel. *Adv. Synth. Catal.*, **351**, 1789 (2009).
- [17] P-H. Li, B-L. Li, Z-M. An, L-P. Mo, Z-S. Cui, Z-H. Zhang. *Adv. Synth. Catal.*, **355**, 2952 (2013).
- [18] S-S. Wang, W. Liu, Q-X. Wan, Y. Liu. *Green Chem.*, **11**, 1589 (2009).
- [19] H.L. Xie, Y.X. Fan, C.H. Zhou, Z.X. Du, E.Z. Min, Z.H. Ge, X.N. Li. *Chem. Biochem. Eng. Q.*, **22**, 25 (2008).
- [20] M. Masteri–Farahani, F. Farzaneh, M. Ghandi. *J. Mol. Catal. A: Chem.*, **248**, 53 (2006).
- [21] L. Zhang, W. Dong, H. Sun. *Nanoscale*, **5**, 7664 (2013).
- [22] S.A. Jadhav, R. Bongiovanni. *Adv. Mat. Lett.*, **3**, 356 (2012).
- [23] J. Sun, G. Yu, L. Liu, Zh. Li, Q. Kan, Q. Huo, J. Guan. *Catal. Sci. Technol.*, **4**, 1246 (2014).
- [24] C. Hui, C. Shen, J. Tian, L. Bao, H. Ding, C. Li, Y. Tian, X. Shi, H-J. Gao. *Nanoscale*, **3**, 701 (2011).
- [25] D. Dupont, J. Luyten, M. Bloemen, T. Verbiest, K. Binnemans. *Ind. Eng. Chem. Res.*, **53**, 15222 (2014).
- [26] L. Wortmann, S. Ilyas, D. Niznansky, M. Valldor, K. Arroub, N. Berger, K. Rahme, J. Holmes, S. Mathur. *Appl. Mater. Interfaces*, **6**, 16631 (2014).
- [27] C. Jin, Y. Wang, H. Wei, H. Tang, X. Liu, T. Lu, J. Wang. *J. Mater. Chem. A*, **2**, 11202 (2014).
- [28] R.K. Sharma, S. Dutta, S. Sharma. *Dalton Trans.*, **44**, 1303 (2015).
- [29] D. Wang, D. Astruc. *Chem. Rev.*, **114**, 6949 (2014).
- [30] Y. Leng, J. Zhao, P. Jiang, J. Wang. *ACS Appl. Mater. Interfaces*, **6**, 5947 (2014).

- [31] G.J.J. Chen, J.W. McDonald, W.E. Newton. *Inorg. Chem.*, **15**, 2612 (1976).
- [32] L. Buzoglu, E. Maltas, M. Ozmen, S. Yildiz. *Colloids Surf. A: Physicochem. Eng. Aspects*, **442**, 139 (2014).
- [33] W. Li, Y. Deng, Z. Wu, X. Qian, J. Yang, Y. Wang, D. Gu, F. Zhang, B. Tu, D. Zhao. *J. Am. Chem. Soc.*, **133**, 15830 (2011).
- [34] W. Wu, Q. He, C. Jiang. *Nanoscale Res. Lett.*, **3**, 397 (2008).
- [35] X. Le, Z. Dong, Z. Jin, Q. Wang, J. Ma. *Catal. Commun.*, **53**, 47 (2014).
- [36] E.B. Seena, M.R. Prathapachandra Kurup. *Polyhedron*, **26**, 3595 (2007).
- [37] V. Vrdoljak, I. Đilović, M. Cindrić, D. Matković-Čalogović, N. Strukan, A. Gojmerac-Ivšić, P. Novak. *Polyhedron*, **28**, 959 (2009).
- [38] Z. Zhang, B. Liu, K. Lv, J. Sun, K. Deng. *Green Chem.*, **16**, 2762 (2014).
- [39] L.J. Laughlin, C.G. Young. *Inorg. Chem.*, **35**, 1050 (1996).
- [40] X. Huang, W. Guo, G. Wang, M. Yang, Q. Wang, X. Zhang, Y. Feng, Z. Shi, C. Li. *Mat. Chem. Phys.*, **135**, 985 (2012).
- [41] R. Rahimi, A. Maleki, S. Maleki, A. Morsali, M.J. Rahimi. *Solid State Sci.*, **28**, 9 (2014).
- [42] F. Galeotti, F. Bertini, G. Scavia, A. Bolognesi. *J. Colloid Interface Sci.*, **360**, 540 (2011).
- [43] M. Bagherzadeh, M. Zare, V. Amani, A. Ellern, L.K. Woo. *Polyhedron*, **53**, 223 (2013).
- [44] H. Mimoun. *Catal. Today*, **1**, 281 (1987).
- [45] P. Ferreira, I.S. Goncalves, F.E. Kühn, A.D. Lopes, M.A. Martins, M. Pillinger, A. Pina, J. Rocha, C.C. Romao, A.M. Santos, T.M. Santos, A.A. Valente. *Eur. J. Inorg. Chem.*, 2263 (2000).

Table 1. Fe<sub>3</sub>O<sub>4</sub>@SiO<sub>2</sub>-NHAlMo catalyzed epoxidation of different olefins by t-BuOOH<sup>a</sup>.

Entry	Substrate	Conversion <sup>b</sup> %	Selectivity <sup>b</sup> %	Time (min)
1 <sup>c</sup>	cyclooctene	26	100	60
2	cyclooctene	98	98	20
3	cyclohexene	98	100	30
4	n-heptene	97	100	30
5	n-octene	94	100	60
6	styrene	99	45	60
7	4-methoxystyrene	50	72	60
8	$\alpha$ -methylstyrene	62	60	60

<sup>a</sup>Reaction condition: 10 mg catalyst: 1 mmol alkene: 1 mmol t-BuOOH. The reactions were run under reflux in 1 mL dichloroethane. <sup>b</sup>GC yield was determined by GC with respect to an internal standard (chlorobenzene). <sup>c</sup>Without the catalyst.

Table 2. Reuses of Fe<sub>3</sub>O<sub>4</sub>@SiO<sub>2</sub>-NHAlMo in the selective oxidation of cyclooctene<sup>a</sup>

Run	Conversion <sup>b</sup> %	Selectivity <sup>b</sup> %
1	98	98
2	99.6	98
3	99.6	98
4	95	98
5	94	98
6	94	98

<sup>a</sup>Reaction condition: 10 mg catalyst: 1 mmol cyclooctene: 1 mmol t-BuOOH. The reactions were run under reflux for 20 min. <sup>b</sup>The conversion and selectivity were determined by GC with respect to an internal standard (chlorobenzene).

ACCEPTED MANUSCRIPT

Table 3. Comparison of the Fe<sub>3</sub>O<sub>4</sub>@SiO<sub>2</sub>-NHAlMo catalytic activity with those of reported molybdenum nanocatalysts.

Entry	Catalyst	Molar ratio cat:sub:ox	Temp. (°C)	Time	Conversion %	Ref.
1	Fe <sub>3</sub> O <sub>4</sub> @SiO <sub>2</sub> -NHAlMo	0.008.:1:1	Reflux	20 min	98	This work
2	Mo-MCM-41	1:68:205	40	3 h	97	11
3	1Mo@SMNP	0.01:1:1.2	Reflux	6 h	96	16
4	2Mo@SMNP	0.01:1:1.2	Reflux	6 h	58	16
5 <sup>a</sup>	Mo-Fe <sub>3</sub> O <sub>4</sub> @SiO <sub>2</sub> @P <sub>4</sub> VP	0.059:3.5:22	60	12 h	85.6	40
6	MCM-41-MoO <sub>2</sub> Cl(THF) <sub>2</sub>	0.082:7.3:11	55	2 h	31	45
7	MCM-41-L/MoO <sub>2</sub> Cl <sub>2</sub>	0.082:7.3:11	55	2 h	29	45

<sup>a</sup>H<sub>2</sub>O<sub>2</sub> has been used as oxidant.

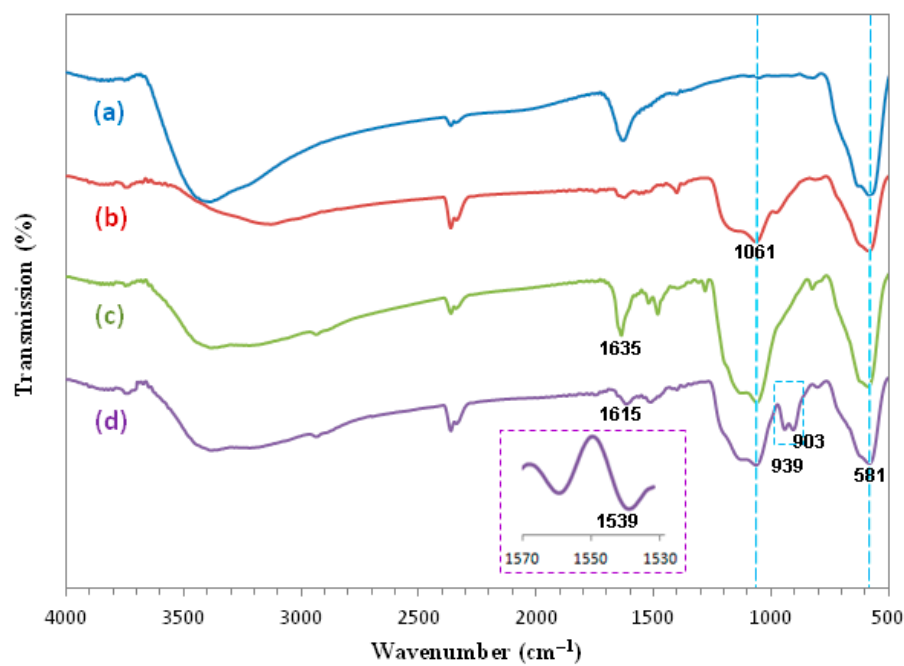


Figure 1. FT-IR spectra of (a)  $\text{Fe}_3\text{O}_4$ , (b)  $\text{Fe}_3\text{O}_4@\text{SiO}_2$ , (c)  $\text{Fe}_3\text{O}_4@\text{SiO}_2\text{-NHAl}$  and (d)  $\text{Fe}_3\text{O}_4@\text{SiO}_2\text{-NHAlMo}$  (inset: high resolution spectrum of 1d).

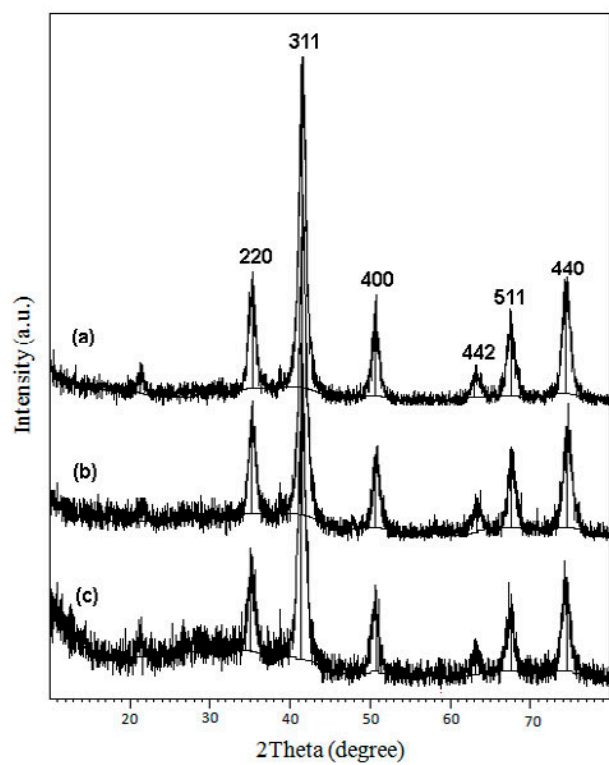


Figure 2. The XRD patterns of (a) Fe<sub>3</sub>O<sub>4</sub>, (b) Fe<sub>3</sub>O<sub>4</sub>@SiO<sub>2</sub>-NHAl and (c) Fe<sub>3</sub>O<sub>4</sub>@SiO<sub>2</sub>-NHAlMo.

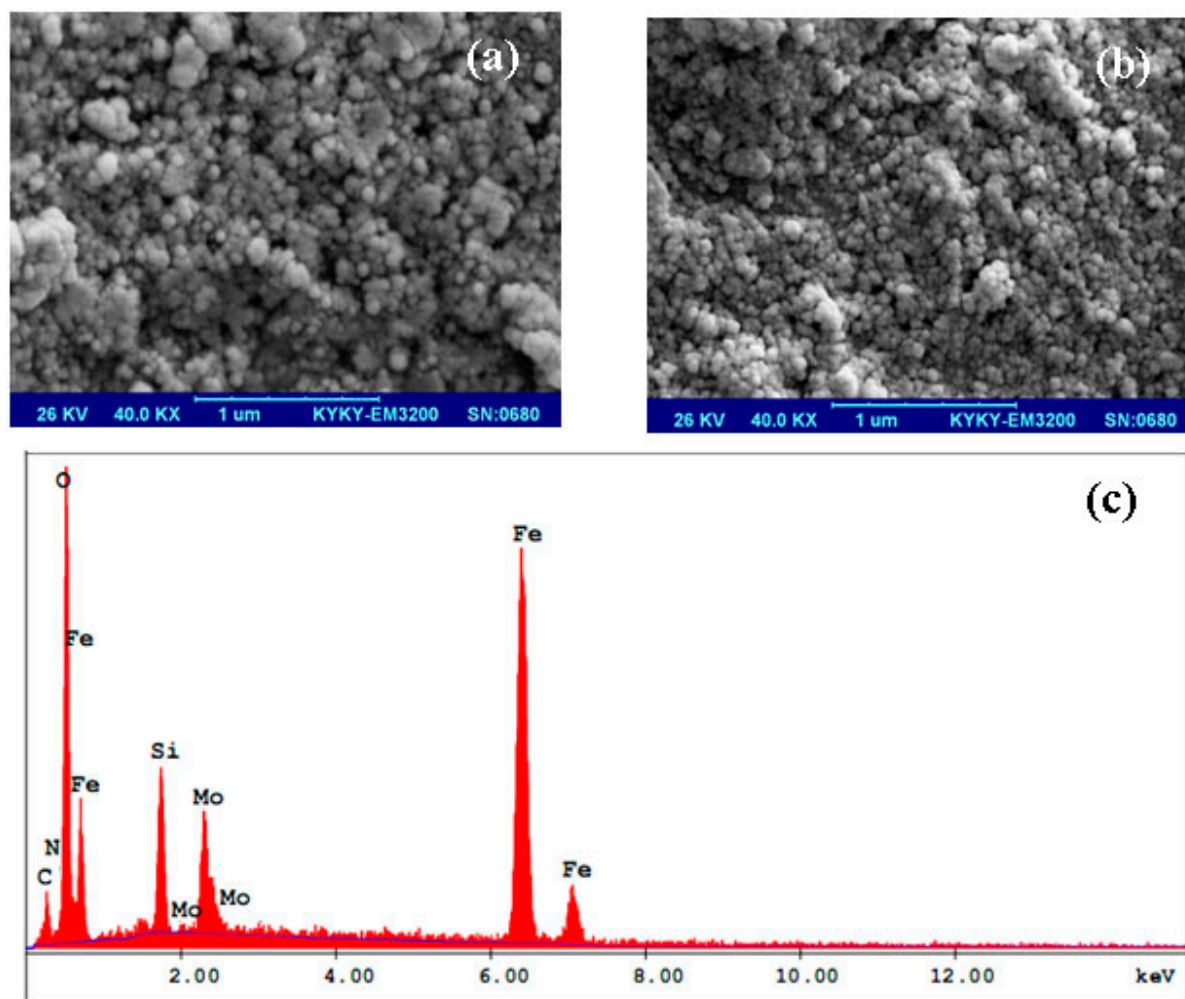


Figure 3. SEM images of (a)  $\text{Fe}_3\text{O}_4$ , (b)  $\text{Fe}_3\text{O}_4@ \text{SiO}_2\text{-NHAlMo}$  and (c) the EDX pattern of  $\text{Fe}_3\text{O}_4@ \text{SiO}_2\text{-NHAlMo}$ .

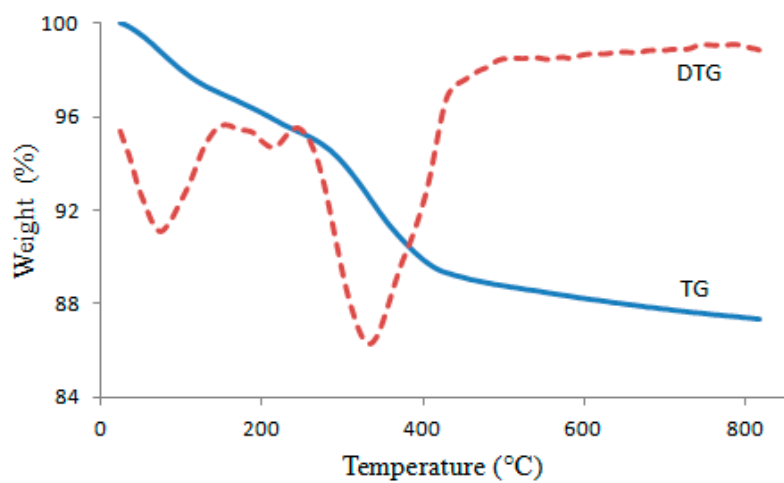


Figure 4. Thermogravimetric curves of  $\text{Fe}_3\text{O}_4@ \text{SiO}_2\text{-NHAlMo}$  nanocomposite.

ACCEPTED MANUSCRIPT

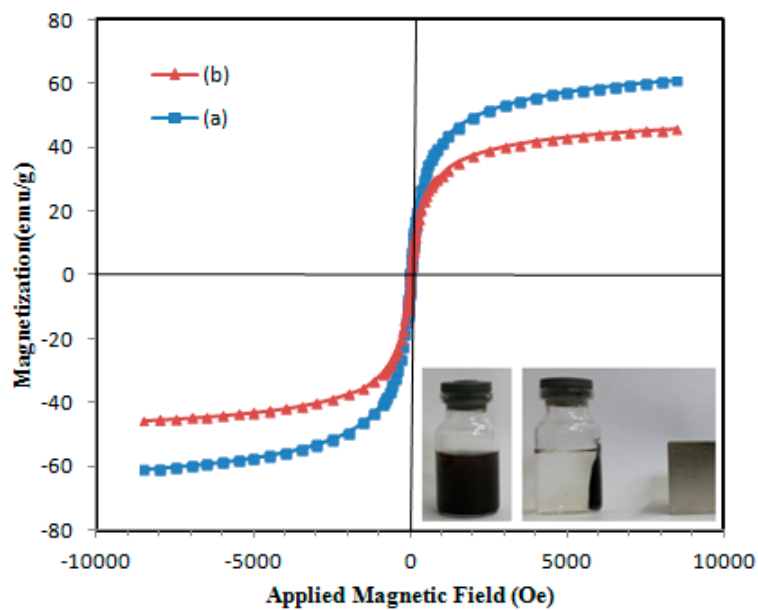


Figure 5. VSM magnetization curves of (a) Fe<sub>3</sub>O<sub>4</sub> microspheres and (b) Fe<sub>3</sub>O<sub>4</sub>@SiO<sub>2</sub>-NHAlMo nanocomposite (inset: photos for magnetic separation of catalyst by external magnet).

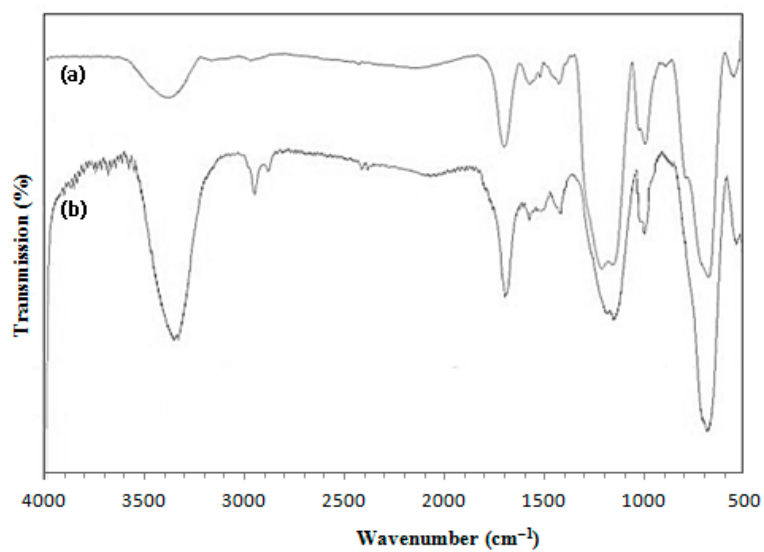
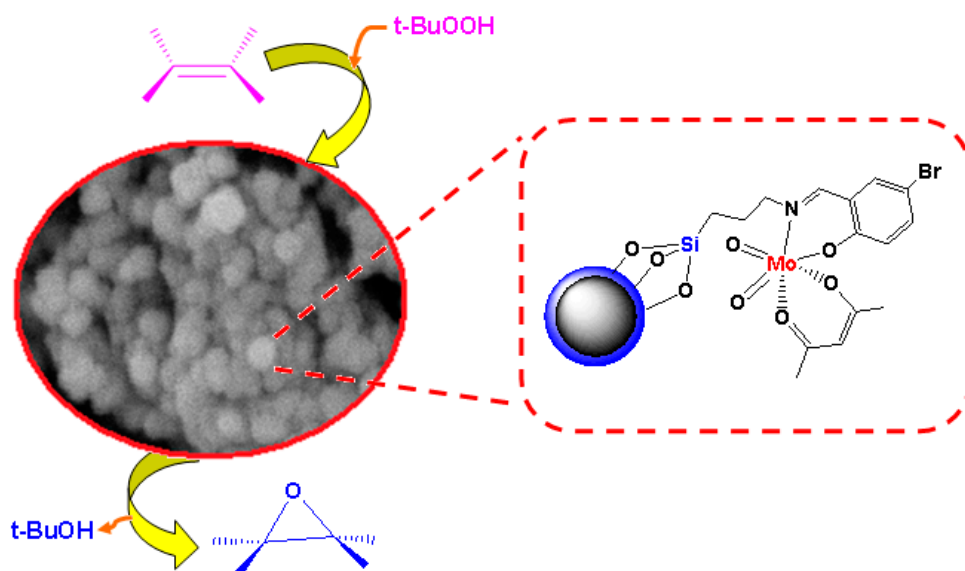


Figure 6. IR spectra of (a) Fe<sub>3</sub>O<sub>4</sub>@SiO<sub>2</sub>-NHAlMo and (b) used catalyst after the 6th cycle.

ACCEPTED MANUSCRIPT

## Graphical abstract



ACCEPTED MANUSCRIPT